

Electronic Journal of Biotechnology ISSN: 0717-3458
<http://www.ejbiotechnology.info>
DOI: 10.2225/vol16-issue5-fulltext-8

RESEARCH ARTICLE

Superparamagnetic Poly (3-hydroxybutyrate-co-3 hydroxyvalerate) (PHBV) nanoparticles for biomedical applications

Cristian Vilos^{1,3} ✉ · Marlen Gutiérrez^{2,3} · Roberto A. Escobar^{2,3} · Francisco Morales¹ · Juliano C. Denardin^{2,3}
· Luis Velasquez^{1,3} · Dora Altbir^{2,3}

1 Universidad Andres Bello, Facultad de Medicina, Center for Integrative Medicine and Innovative Science, Santiago, Chile

2 Universidad de Santiago de Chile, Facultad de Ciencia, Departamento de Física, Santiago, Chile

3 Center for the Development of Nanoscience and Nanotechnology, Santiago, Chile

✉ Corresponding author: cristian.vilos@unab.cl
Received March 21, 2013 / Accepted July 30, 2013
Published online: September 15, 2013
© 2013 by Pontificia Universidad Católica de Valparaíso, Chile

Abstract

Background: The progress in material science and the recent advances in biodegradable/biocompatible polymers and magnetic iron oxide nanoparticles have led to develop innovative diagnostic and therapeutic strategies for diseases based on multifunctional nanoparticles, which include contrast medium for magnetic resonance imaging, agent for hyperthermia and nanocarriers for targeted drug delivery. The aim of this work is to synthesize and characterize superparamagnetic iron oxide (magnetite), and to encapsulate them into poly (3-hydroxybutyrate-co-3-hydroxyvalerate) (PHBV) nanoparticles for biomedical applications.

Results: The magnetite nanoparticles were confirmed by X-ray diffraction and exhibited a size of 22.3 ± 8.8 nm measured by transmission electron microscopy (TEM). Polymeric PHBV nanoparticles loaded with magnetite (MgNPs) were analyzed using dynamic light scattering and showed a size of 258.6 ± 35.7 nm and a negative zeta potential (-10.8 ± 3.5 mV). The TEM examination of MgNPs exhibited a spherical core-shell structure and the magnetic measurements showed in both, non-encapsulated magnetite and MgNPs, a superparamagnetic performance. Finally, the *in vitro* studies about the magnetic retention of MgNPs in a segment of small intestine of rats showed an active accumulation in the region of the magnetic field.

Conclusions: The results obtained make the MgNPs suitable as potential magnetic resonance imaging contrast agents, also promoting hyperthermia and even as potential nanocarriers for site-specific transport and delivery of drugs.

Keywords: hyperthermia, magnetic resonance image (MRI), magnetite, PHBV, polymeric nanoparticles.

INTRODUCTION

Magnetic nanoparticles provide a multifunctional platform for scientific and clinical applications, such as biosensors, protein and cell separation systems and magnetic carriers for hyperthermia and tissue-specific drug delivery (Gao et al. 2009). Iron oxide nanoparticles are highly biocompatible in the body because the iron uptake, transport and storage in the liver are highly regulated by proteins such as ferritin and transferrin (Corchero and Villaverde, 2009). On the other hand, iron oxide nanoparticles are cleared efficiently from the body and do not induce oxidative stress or long-term changes in liver enzyme levels (Jain et al. 2008). In addition, Fe-based nanoparticles, such as magnetite (Fe_3O_4) and maghemite ($\gamma\text{-Fe}_2\text{O}_3$), exhibit lower toxicity and less susceptibility to oxidation than other magnetic

materials with high magnetic moments, such as cobalt and nickel making them suitable for diagnostic and therapeutic strategies (Sanvicens and Marco, 2008).

The magnetic resonance imaging (MRI) as a non-radiating biomedical imaging technique has shown advantages over others strategies used to elucidate the evolution and progression of different pathologies, which include brain aneurysms, stroke, and breast, brain, and prostate tumors (Cormode et al. 2009). Gadolinium is the most used contrast agent for MRI; however, magnetite nanoparticles have recently been extensively tested as contrast agents for MRI because their magnetic susceptibility is higher than that of gadolinium chelates, and their magnetic properties alters the relaxation times T2 of the resonance (Haw et al. 2010). An example of these nanoparticles is GastroMARK[®], which is a commercial MRI contrast agent comprising silicone-coated superparamagnetic iron oxide nanoparticles. GastroMARK[®] allows to obtain images with an enhance delineation of the bowel, which makes it distinguished from organs and tissues that are adjacent of the gastrointestinal tract.

The magnetic characterization of particles is determined by measuring their response to an external magnetic field, H_a . If we consider a system composed of several nanoparticles small enough such that each is a monodomain with negligible anisotropy, it is possible for the thermal energy, $K_B T$, to become higher than or equal to the activation energy. In this case, the particle can orient its magnetization along any direction, thereby, losing its magnetic stability (Xu and Sun, 2009). If the direction of the magnetization changes several times during a measurement, then the measured magnetization will be zero at zero external fields. This effect, known as superparamagnetism, is fundamental to many biological applications (Lee et al. 2009). Superparamagnetic particles respond rapidly to an external field, which allows the relaxation time to be varied. In nuclear MRI, the images exhibit a resonant response to an alternating magnetic field, which can be used to heat up the surrounding tissue by energy transfer and generate hyperthermia. Thus, nuclear MRI is a promising tool for cancer therapy (Kim et al. 2009).

The application of magnetic nanoparticles as contrast agents for MRI depends on their properties, such as magnetic susceptibility, superparamagnetic performance, and biocompatibility with specific biomedical applications. Magnetite nanoparticles are not stable in an environment with abundant oxygen, because Fe^{2+} ions are oxidized to iron oxyhydroxides, losing their original magnetic properties.

The development of biocompatible and biodegradable polymers has provided a robust platform to create innovative diagnostic and therapeutic strategies based on micro and nanoparticles (Shi et al. 2011; Vilos and Velásquez, 2012). The polymeric nanoparticles as drug delivery system have shown suitable physical and mechanical properties, which can be easily modified, enabling control of the pharmacokinetic and biodistribution of drugs (Tekade and Gattani, 2009). Poly (D, L lactide-co-glycolide), poly (sebacic anhydride) and poly (ϵ -caprolactone) are some of the most commonly used polymers in biomedicine (Pillai and Panchagnula, 2001). The poly (3-hydroxybutyrate-co-3-hydroxyvalerate) (PHBV) is a biodegradable and biocompatible polymer that has shown useful properties for drug delivery and tissue engineering (Vilos et al. 2012; Vilos et al. 2013). PHBV is cost-effective and has physicochemical properties similar to those of the most widely used polymers (Holmes, 1985). In this study, we synthesized and characterized iron oxide (magnetite), formulated magnetite-loaded PHBV nanoparticles, and examined their magnetic properties as putative MRI contrast agents for hyperthermia induction and tissue-specific drug delivery.

MATERIALS AND METHODS

The aqueous suspension of silicone-coated, superparamagnetic iron oxide (GastroMARK[®]) was purchased from AMAG Pharmaceuticals, Inc. (Lexington, MA, USA). An ultrasonic processor, VCX 130 PB (Sonics Inc.; Newtown, CT, USA) fitted with a microtip Ti-6Al-4V probe was used to synthesize the iron oxide-loaded polymeric nanoparticles. PHBV (12 wt.% PHV content) and polyvinyl alcohol (PVA, MW 30,000-70,000) were purchased from Sigma-Aldrich (St. Louis, MO, USA). Analytical grade dichloromethane (DCM), methanol, and solution ammonia ($NH_{3(aq)}$), iron (II) chloride tetrahydrate ($FeCl_2 \times 4H_2O$), iron (III) chloride hexahydrate ($FeCl_3 \times 6H_2O$), and potassium nitrate (KNO_3) were purchased from Merck (Darmstadt, Germany).

Synthesis of magnetite

The synthesis method used has been widely reported (Nedkova et al. 2006; Frimpong et al. 2010; Utkan et al. 2011). Iron oxides (either Fe_3O_4 or $\delta\text{-Fe}_2\text{O}_3$) can be synthesized through the co-precipitation of Fe^{2+} and Fe^{3+} aqueous salt solutions by addition of a base. The control of size, shape and composition of nanoparticles depends on the type of salts used (e.g. chlorides, sulphates, nitrates, perchlorates, etc.), Fe^{2+} and Fe^{3+} ratio, pH and ionic strength of the media. We use the co-precipitation method described by Gupta and Gupta (2005) and modifications by Gutiérrez et al. (2010) to obtain superparamagnetic magnetite nanoparticles. We mixed a FeCl_2 and FeCl_3 solutions (1 M) in a 1:2 molar ratio. After these processes we added $\text{Na}_3\text{C}_3\text{H}_5\text{O}(\text{COO})_3$ (0.3 M). The final solution was mixed during 1 hr at room temperature (298 K) in a N_2 atmosphere. The precipitate was washed to eliminate salts excess.

Preparation of magnetite-loaded PHBV nanoparticles

A modification of the double emulsion water-in-oil-in-water ($W_1/O_1/W_2$) evaporation method described by Gomez-Lopera (2001) was used to develop colloidal magnetite-loaded nanoparticles (MgNPs) (Figure 1). Experimentally, a first water-in-oil (W_1/O_1) emulsion was prepared by the incorporation of 300 μL of an aqueous solution of magnetite (0.5 mg/mL) in 1 mL of PHBV solution (25 mg/mL) in DCM using an ultrasonic processor equipped with a microtip probe for 60 sec at 125 W in an ice bath because the microtip produces an exothermal reaction. This emulsion was added to 4 mL of an aqueous solution of PVA (1% w/v), and was sonicated for 60 sec at 125 W in an ice bath to obtain the second emulsion ($W_1/O_1/W_2$). The second emulsion was immediately poured into a beaker containing 20 mL of PVA solution (0.1% w/v), and stirred for 12 hrs to evaporate the DCM. Finally, the solidified magnetite-loaded PHBV nanoparticles were harvested by centrifugation at 11,000 rpm for 30 min and washed three times with distilled water and either stored at 4°C for immediate use, or lyophilized and storage at -80°C for posterior use. The concentration of magnetite added to MgNPs was equivalent to that specified by the commercial MRI contrast agent GastroMARK[®].

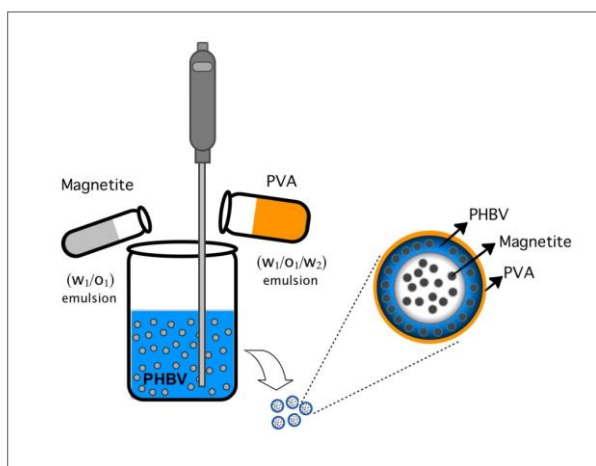


Fig. 1 Schematic representation of the double emulsion method used to formulate MgNPs. A first water-in-oil emulsion (w_1/o_1) is generating by incorporation of magnetite dissolved in water (gray vial) in an amount of PHBV dissolved in dichloromethane (blue vial) by sonication until to obtain a homogeneous phase. This first emulsion after is added to a larger volume polyvinyl alcohol (PVA) (orange vial) and sonicated to get a second emulsion ($w_1/o_1/w_2$). The PVA is an aqueous solution that provides stabilization to the nanoparticles. Finally, these emulsions are arranged in a shaker system during 12 hrs to evaporate the solvent and solidified the nanoparticles, which after are washed by centrifugation and either stored at 4°C for immediate use, or lyophilized and storage at -80°C .

CHARACTERIZATION

X-ray diffraction (XRD) of magnetite

Magnetite nanoparticles were identified by comparing the X-ray diffraction (XRD) patterns obtained from randomly oriented powder mounts with a Philips X'Pert diffractometer (graphite-monochromated Cu-K α radiation) and ICDD-PDF data.

Analysis by electronic transmission microscopy (TEM)

The magnetite particles and MgNPs were characterized by transmission electron microscopy (TEM) (Phillips-TECNAI 12 BIOTWIN EM Microscope, FEI Company, Hillsboro, OR). The samples of magnetite were prepared by depositing 0.1 mL of the magnetite suspension (1.0 mg/mL) onto a 300-mesh carbon-coated copper grid. The diameter of magnetite nanoparticles was determined by analyzing five images from three independent samples using the Image J software (NIH). In the case of MgNP, the samples were prepared by depositing 0.1 mL of the MgNP suspension (1.0 mg/mL) onto a 300-mesh carbon-coated copper grid, and negatively stained for 5 min at room temperature with freshly prepared and sterile-filtered aqueous uranyl acetate solution (2% w/v). The grids were washed with distilled water prior to imaging. All samples were analyzed at 80 kV with an acceleration voltage of 200 kV.

Size and zeta potential of MgNPs

The size, in nm, and zeta potential, in mV, of the MgNPs were evaluated using Dynamic light scattering (DLS). The samples were suspended in 1 mL of PBS (phosphate buffered saline) at pH 7.4, and analyzed at 298 K (room temperature) in a Zetasizer 3000 (Malvern Instruments, UK). The results obtained were calculated from three independent experiments.

Magnetic measurements

The magnetic properties of the magnetite and MgNPs were compared with those of GastroMARK[®] (Ferumoxsil, oral suspension). Magnetic measurements were carried out using a vibrating sample magnetometer (VSM), and the hysteresis loop was measured at 300 K as a function of an external applied field, H_a .

Magnetic accumulation of MgNPs in intestinal tissue

Fluorescent MgNPs were prepared with the same protocol used to formulate the magnetite-loaded PHBV nanoparticles by the incorporation of Alexa Fluor[®] 488 dye (Catalogue Number, A32750, Molecular Probes-Invitrogen, Carlsbad, CA) in the aqueous phase of the first emulsion. The accumulation magnetic nanoparticles were analyzed in segments of the small intestine of rats under the presence and absence of an applied magnetic field.

Six male adult Sprague-Dawley rats (Central Vivarium of the Faculty of Medicine, University of Chile, Santiago, Chile) weighing 200-250 g were separated in two groups: experimental ($n = 3$) and control ($n = 3$). The animals were housed 3 per cage, kept in a room temperature and light-controlled environment (12:12 hrs, light: dark cycle with lights on at 7.00 AM) and had *ad libitum* access to food and water. The housing conditions and experimental procedures follow the protocols approved by the Bioethics Committee of Universidad Andrés Bello, and in accordance with the "Guide for Care and Use of Laboratory Animals" published by the U.S. National Institutes of Health.

Experimentally, two segments of 3 cm length of the small intestine of each animal were obtained by surgical procedures after sacrificing by anaesthetic overdose of isoflurane, and the samples were separated in two groups (experimental and control). In the experimental group, a cylindrical neodymium magnet (4.540 gauss) of 6 mm x 6 mm was fixed in the middle portion of the small intestine using LiquiVet tissue-adhesive (Oasis Medical Mettawa, Illinois, USA), while no magnetic field was applied to the control group. The samples were washed three times with 1 mL of phosphate buffered saline (PBS), pH 7.4 (0.14 M sodium chloride, 0.003 M potassium chloride, 0.002 M

potassium phosphate, 0.01 M sodium phosphate) and then were inoculated with 100 μL of suspension of 6 mg/mL of alexa fluor-loaded magnetic nanoparticles (af-MgNPs). Finally, samples were washed ten times with 1 mL of PBS (pH 7.4), and the accumulation of fluorescent nanoparticles in the tissue was analyzed in the iBox Scientia Small Animal Imaging System (Upland, CA, USA).

RESULTS AND DISCUSSION

Superparamagnetic iron oxide nanoparticles

Iron oxide particles were synthesized using a co-precipitation method, which is a highly reproducible technique that generates particles that are almost uniform in size. The XRD results (Figure 2) showed a typical magnetite (Fe_3O_4) pattern with an interplanar spacing (d) of 4.84, 2.97, 2.53, 2.42, 2.10, 1.71, 1.62, and 1.48 \AA . When compared with the reflection ICDD-PDF card # 01-085-1436, these peaks confirmed the exclusive presence of magnetite. TEM analysis revealed spherical particles with a diameter of 22.3 ± 8.8 nm (Figure 3a). Even considering their small size, these results suggest that the magnetite particles show superparamagnetic behaviour.

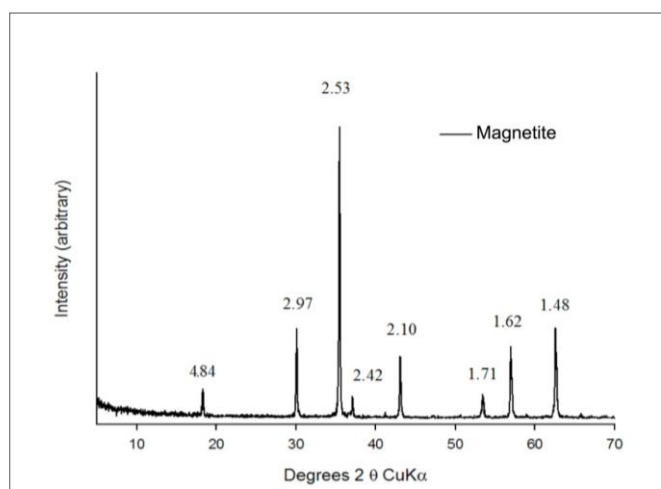


Fig. 2 X-ray Diffraction (XRD) of synthesized magnetite. Numbers indicate the d -values (\AA) of interplanar spacing. The patterns obtained were compared with the reflection ICDD-PDF card # 01-085-1436, which confirmed the sole presence of magnetite.

Magnetite-loaded PHBV nanoparticles (MgNPs)

The MgNPs were formulated using a modified double-emulsion evaporation method. Prior, the synthetic magnetite particles obtained by co-precipitation were efficiently suspended in water and incorporated in the aqueous phase of the first emulsion. The rational design of MgNPs comprised the use of PVA as an emulsifier and stabilizing agent. PVA confers remarkably low cytotoxicity and a negative zeta potential to nanoparticles (DeMerlis and Schoneker, 2003; Roy et al. 2010; Dong et al. 2011). Charges on the nanoparticle surface produce repulsive electrostatic forces that prevent aggregation and help to stabilize the suspension (Min et al. 2008). In addition, the negative charge of the nanoparticles is particularly useful for biomedical applications, because positively charged micro and nanoparticles stimulate their uptake by monocytes and macrophages, thereby decreasing their bioavailability (Nel et al. 2009). The zeta potential of MgNPs was determined in a Zetasizer 3000 and exhibited -10.8 ± 3.5 mV. The negative zeta potential of MgNPs was consistent with other studies that used PVA as an emulsifier and stabilizing agent (Liu et al. 2007; Zhao et al. 2007). It was not possible to characterize MgNPs by XRD because magnetite content in the sample is below the detection limit of this technique (less than 5%). Because the polymer is not crystalline, the signal obtained is part of the noise of the measurement.

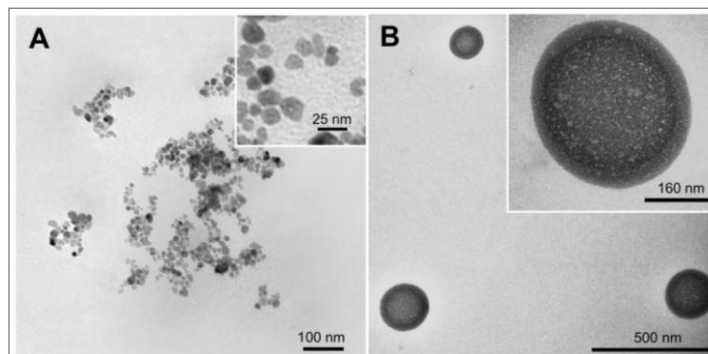


Fig. 3 Transmission electron microscopy (TEM) of magnetite and MgNPs. (a) Magnetite. (b) MgNPs stained with uranyl acetate solution, which enhances the electron density of hydrophilic areas. The MgNPs showed a core-shell structure (polymer-hollow) and a uniform inner magnetite load.

Size of MgNPs

The analysis by dynamic light scattering (DLS) of MgNPs showed a size (diameter, nm) of 258.6 ± 35.7 nm as shown in Figure 4. These results could support to use the MgNPs in medical applications, particularly those related to cancer diagnosis and/or treatment, because nanoparticles ranging 10-500 nm in diameter can extravasate (escape from the blood vessels) into tumour tissues due to passive targeting by the enhanced permeation and retention (EPR) phenomenon. EPR is essential for tumour growth, as it provides an adequate supply of oxygen and nutrients (Maeda, 2001). On the other hand, the size distribution of the MgNPs was uniform, as previously reported by other authors using similar procedures to formulate nanoparticles (Yang et al. 2006; Liu, et al. 2007). However, the average diameter of MgNPs was smaller than the commercial product based on magnetite covered with silicone (GastroMARK[®]) which has about ~400 nm in diameter.

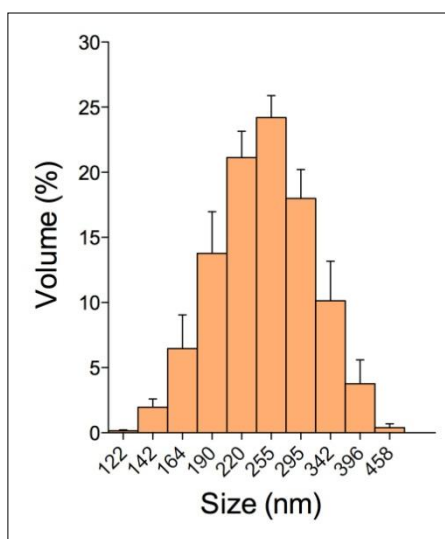


Fig. 4 Size distribution of MgNPs obtained by dynamic light scattering (DLS). The average diameter of the MgNPs was 258.6 ± 35.7 nm.

Analysis by transmission electron microscopy

TEM examination of MgNPs revealed spherical nanosized nanoparticles comprising a core-shell structure, and three layers with different electron densities. The external layer represented the PHBV

polymer and had a thickness of approximately 30 to 40 nm; the layer at the polymer-core interface showed a higher concentration of magnetite; and the inner core contained an almost homogeneous distribution of magnetite. In addition, the negative staining by uranyl acetate, which increases the contrast of hydrophilic structures, exhibited that the interface core-PHBV display the most hydrophilic structure inside of MgNPs, being a putative site for load water soluble drugs, and the PHBV polymeric layer for hydrophobic drugs (Figure 3b).

Magnetite inside the MgNPs exhibited a more uniform distribution than previous formulations based on the PLGA polymer or those obtained using a similar double emulsion method (Ngaboni Okassa et al. 2005; Wang et al. 2008). This is important for biomedical applications where the size control is crucial. Therefore a more uniform size distribution represents a narrower magnetization distribution and thus a reproducible magnetic response.

Magnetic characterization

The magnetic characterization of magnetite non-encapsulated (Fe_3O_4) and MgNPs was carried out in a vibrating sample magnetometer (VSM). The magnetic properties of the synthesized magnetite and MgNPs were compared with those of GastroMARK[®]. The hysteresis loops (Figure 5) showed a saturation of approximately 8 emu/g for magnetite and 6 emu/g for MgNPs. These results were higher than those for GastroMARK[®] (2 emu/g). Magnetite and MgNPs exhibited neither remanence nor coercivity, confirming their superparamagnetic behaviour. The differences in saturation values between MgNPs and magnetite are due to the difference in concentration of magnetic material present in each sample.

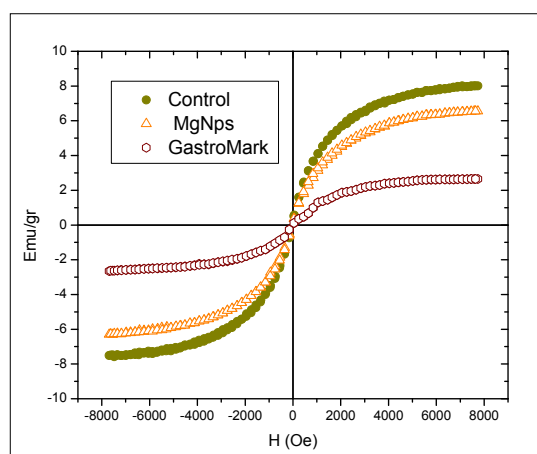


Fig. 5 Hysteresis loops of magnetite, MgNPs, and GastroMARK[®] obtained with a vibrating magnetometer (VSM) at room temperature as a function of the external field.

Magnetic accumulation in intestinal tissue

The tissue-accumulation of alexa fluor-loaded magnetic nanoparticles (af-MgNPs) was assessed in segments of the small intestine of rats in the presence and absence of a magnetic field adhered to the serous membrane of intestinal tissue. The results showed in Figure 6 exhibits a significant accumulation of af-MgNPs in the segments of the small intestine in presence of a magnet fixed in the middle portion, which support their use as nanocarrier to site-specific delivery of drug. In addition, the biodegradable/biocompatible polymeric structure of MgNPs and their superparamagnetic character make them promising candidates for theranostic purposes as MRI contrast agents and for the induction of electromagnetic hyperthermia.

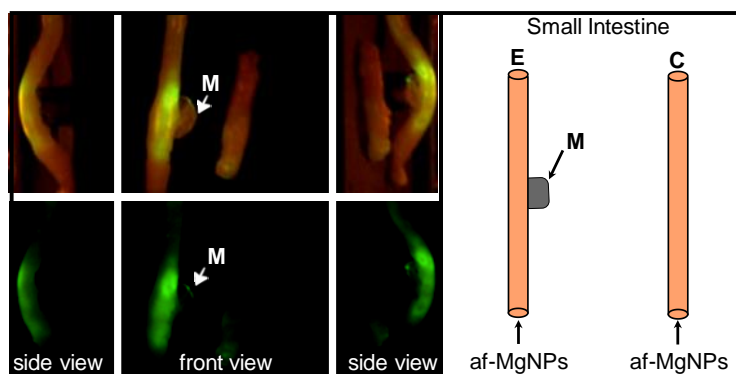


Fig. 6 Magnetic accumulation of alexa fluor-loaded magnetic nanoparticles (af-MgNPs) in a segment of the small intestine with a cylindrical neodymium magnet (M) (4.540 gauss, 6 x 6 mm) and visualized by an animal imaging system. Experimental (E) and control (C) groups.

CONCLUDING REMARKS

In this study, we report the synthesis and characterization of magnetite and magnetite-loaded PHBV nanoparticles (MgNPs) for biomedical applications. The MgNPs showed an average size of ~250 nm, a spherical shape with a core-shell structure, and homogenous inner distribution of magnetite. Magnetic characterization by VSM shows the superparamagnetic behaviour of magnetite, MgNPs synthesized and MRI contrast agent GastroMARK[®]. Such magnetic property makes MgNPs a suitable system as MRI contrast agent and even could be used in experimental hyperthermia treatment. Finally, the *in vitro* tissue-retention analysis suggests that MgNPs promise as site-specific nanocarriers of drug.

Financial support: This work was partially supported by FONDECYT under projects 1120356, 1110252, Millennium Science Nucleus Basic and Applied Magnetism No. P06-022F, Financiamiento Basal para Centros Científicos y Tecnológicos de Excelencia No. FB0807. R.A. Escobar acknowledges a fellowship from CONICYT (Chile).

REFERENCES

- CORCHERO, J.L. and VILLAVERDE, A. (2009). Biomedical applications of distally controlled magnetic nanoparticles. *Trends in Biotechnology*, vol. 27, no. 8, p. 468-476. [\[CrossRef\]](#)
- CORMODE, D.P.; SKAJAA, T.; FAYAD, Z.A. and MULDER, W.J.M. (2009). Nanotechnology in medical imaging: Probe design and applications. *Arteriosclerosis Thrombosis and Vascular Biology*, vol. 29, no. 7, p. 992-1000. [\[CrossRef\]](#)
- DEMERLIS, C.C. and SCHONEKER, D.R. (2003). Review of the oral toxicity of polyvinyl alcohol (PVA). *Food and Chemical Toxicology*, vol. 41, no. 3, p. 319-326. [\[CrossRef\]](#)
- DONG, Z.; XIE, S.; ZHU, L.; WANG, Y.; WANG, X. and ZHOU, W. (2011). Preparation and *in vitro*, *in vivo* evaluations of norfloxacin-loaded solid lipid nanoparticles for oral delivery. *Drug Delivery*, vol. 18, no. 6, p. 441-450. [\[CrossRef\]](#)
- FRIMPONG, R.A.; DOU, J.; PECHAN, M. and HILT, J.Z. (2010). Enhancing remote controlled heating characteristics in hydrophilic magnetite nanoparticles via facile co-precipitation. *Journal of Magnetism and Magnetic Materials*, vol. 322, no. 3, p. 326-331. [\[CrossRef\]](#)
- GAO, J.; GU, H. and XU, B. (2009). Multifunctional magnetic nanoparticles: Design, synthesis, and biomedical applications. *Accounts of Chemical Research*, vol. 42, no. 8, p. 1097-1107. [\[CrossRef\]](#)
- GOMEZ-LOPERA, S.A.; PLAZA, R.C. and DELGADO, A.V. (2001). Synthesis and characterization of spherical magnetite/biodegradable polymer composite particles. *Journal of Colloid and Interface Science*, vol. 240, no. 1, p. 40-47. [\[CrossRef\]](#)
- GUPTA, A.K. and GUPTA, M. (2005). Synthesis and surface engineering of iron oxide nanoparticles for biomedical applications. *Biomaterials*, vol. 26, no. 18, p. 3995-4021. [\[CrossRef\]](#)
- GUTIÉRREZ, M.; ESCUDEY, M.; ESCRIG, J.; DENARDIN, J.C.; ALTBIR, D.; FABRIS, J.D.; CAVALCANTE, L.C.D. and GARCÍA-GONZÁLEZ, M.T. (2010). Preparation and characterization of magnetic composites based on a natural zeolite. *Clays and Clay Minerals*, vol. 58, no. 5, p. 589-595. [\[CrossRef\]](#)

- HAW, C.Y.; MOHAMED, F.; CHIA, C.H.; RADIMAN, S.; ZAKARIA, S.; HUANG, N.M. and LIM, H.N. (2010). Hydrothermal synthesis of magnetite nanoparticles as MRI contrast agents. *Ceramics International*, vol. 36, no. 4, p. 1417-1422. [\[CrossRef\]](#)
- HOLMES, P.A. (1985). Applications of PHB-a microbially produced biodegradable thermoplastic. *Physics in Technology*, vol. 16, no. 1, p. 32-36. [\[CrossRef\]](#)
- JAIN, T.K.; REDDY, M.K.; MORALES, M.A.; LESLIE-PELECKY, D.L. and LABHASETWAR, V. (2008). Biodistribution, clearance, and biocompatibility of iron oxide magnetic nanoparticles in rats. *Molecular Pharmaceutics*, vol. 5, no. 2, p. 316-327. [\[CrossRef\]](#)
- KIM, D.; LEE, N.; PARK, M.; KIM, B.H.; AN, K. and HYEON, T. (2009). Synthesis of uniform ferrimagnetic magnetite nanocubes. *Journal of the American Chemical Society*, vol. 131, no. 2, p. 454-455. [\[CrossRef\]](#)
- LEE, C.M.; JEONG, H.J.; KIM, E.M.; KIM, D.W.; LIM, S.T.; KIM, H.T.; PARK, I.K.; JEONG, Y.Y.; KIM, J.W. and SOHN, M.H. (2009). Superparamagnetic iron oxide nanoparticles as a dual imaging probe for targeting hepatocytes *in vivo*. *Magnetic Resonance Medicine*, vol. 62, no. 6, p. 1440-1446. [\[CrossRef\]](#)
- LIU, X.; KAMINSKI, M.D.; CHEN, H.; TORNO, M.; TAYLOR, L. and ROSENGART, A.J. (2007). Synthesis and characterization of highly-magnetic biodegradable poly (D,L-lactide-co-glycolide) nanospheres. *Journal Controlled Release*, vol. 119, no. 1, p. 52-58. [\[CrossRef\]](#)
- MAEDA, H. (2001). The enhanced permeability and retention (EPR) effect in tumor vasculature: The key role of tumor-selective macromolecular drug targeting. *Advances in Enzyme Regulation*, vol. 41, no. 1, p. 189-207. [\[CrossRef\]](#)
- MIN, Y.; AKBULUT, M.; KRISTIANSEN, K.; GOLAN, Y. and ISRAELACHVILI, J. (2008). The role of interparticle and external forces in nanoparticle assembly. *Nature Materials*, vol. 7, no. 7, p. 527-538. [\[CrossRef\]](#)
- NEDKOV, I.; MERODIISKA, T.; SLAVOV, L.; VANDENBERGHE, R.E.; KUSANO, Y. and TAKADA, J. (2006). Surface oxidation, size and shape of nano-sized magnetite obtained by co-precipitation. *Journal of Magnetism and Magnetic Materials*, vol. 300, no. 2, p. 358-367. [\[CrossRef\]](#)
- NEL, A.E.; MADLER, L.; VELEGOL, D.; XIA, T.; HOEK, E.M.V.; SOMASUNDARAN, P.; KLAESSIG, F.; CASTRANOVA, V. and THOMPSON, M. (2009). Understanding biophysicochemical interactions at the nano-bio interface. *Nature Materials*, vol. 8, no. 7, p. 543-557. [\[CrossRef\]](#)
- NGABONI OKASSA, L.; MARCHAIS, H.; DOUZIECH-EYROLLES, L.; COHEN-JONATHAN, S.; SOUCÉ, M.; DUBOIS, P. and CHOURPA, I. (2005). Development and characterization of sub-micron poly (D, L-lactide-co-glycolide) particles loaded with magnetite/maghemite nanoparticles. *International Journal of Pharmaceutics*, vol. 302, no. 1-2, p. 187-196. [\[CrossRef\]](#)
- PILLAI, O. and PANCHAGNULA, R. (2001). Polymers in drug delivery. *Current Opinion Chemical Biology*, vol. 5, no. 4, p. 447-451. [\[CrossRef\]](#)
- ROY, P.; DAS, S.; BERA, T.; MONDOL, S. and MUKHERJEE, A. (2010). Andrographolide nanoparticles in leishmaniasis: Characterization and *in vitro* evaluations. *International Journal of Nanomedicine*, vol. 5, p. 1113-1121. [\[CrossRef\]](#)
- SANVICENS, N. and MARCO, M.P. (2008). Multifunctional nanoparticles - properties and prospects for their use in human medicine. *Trends Biotechnology*, vol. 26, no. 8, p. 425-433. [\[CrossRef\]](#)
- SHI, J.; XIAO, Z.; VOTRUBA, A.R.; VILOS, C. and FAROKHZAD, O.C. (2011). Differentially charged hollow core/shell lipid-polymer-lipid hybrid nanoparticles for small interfering RNA delivery. *Angewandte Chemie-International Edition*, vol. 50, no. 31, p. 7027-7031. [\[CrossRef\]](#)
- TEKADE, A.R. and GATTANI, S.G. (2009). Development and evaluation of pulsatile drug delivery system using novel polymer. *Pharmaceutical Development and Technology*, vol. 14, no. 4, p. 380-387. [\[CrossRef\]](#)
- UTKAN, G.G.; SAYAR, F.; BATAT, P.; IDE, S.; KRIECHBAUM, M. and PISKIN, E. (2011). Synthesis and characterization of nanomagnetite particles and their polymer coated forms. *Journal of Colloid Interface Science*, vol. 353, no. 2, p. 372-379. [\[CrossRef\]](#)
- VILOS, C. and VELÁSQUEZ, L.A. (2012). Therapeutic strategies based on polymeric microparticles. *Journal of Biomedicine and Biotechnology*, no. 672760, p. 1-9. [\[CrossRef\]](#)
- VILOS, C.; STANDIL, L.; HERRERA, N.; SOLAR, P.; ESCOBAR-FICA, J. and VELÁSQUEZ, L.A. (2012). Ceftiofur-loaded PHBV microparticles: A potential formulation for a long-acting antibiotic to treat animal infections. *Electronic Journal of Biotechnology*, vol. 15, no. 4. [\[CrossRef\]](#)
- VILOS, C.; MORALES, F.A.; SOLAR, P.A.; HERRERA, N.S.; GONZALEZ-NILO, F.D.; AGUAYO, D.A.; MENDOZA, H.L.; COMER, J.; BRAVO, M.L.; GONZÁLEZ, P.A.; KATO, S.; CUELLO, M.A.; ALONSO, C.; BRAVO, E.J.; BUSTAMANTE, E.I.; OWEN, G.I. and VELÁSQUEZ, L.A. (2013). Paclitaxel-PHBV nanoparticles and their toxicity to endometrial and primary ovarian cancer cells. *Biomaterials*, vol. 34, no. 16, p. 4098-4108. [\[CrossRef\]](#)
- WANG, Y.; NG, Y.W.; CHEN, Y.; SHUTER, B.; YI, J.; DING, J.; WANG, S.C. and FENG, S.S. (2008). Formulation of superparamagnetic iron oxides by nanoparticles of biodegradable polymers for magnetic resonance imaging. *Advanced Functional Materials*, vol. 18, no. 2, p. 308-318. [\[CrossRef\]](#)
- XU, C. and SUN, S. (2009). Superparamagnetic nanoparticles as targeted probes for diagnostic and therapeutic applications. *Dalton Transactions*, no. 29, p. 5583-5591. [\[CrossRef\]](#)
- YANG, J.; PARK, S.B.; YOON, H.G.; HUH, Y.M. and HAAM, S. (2006). Preparation of poly ϵ -caprolactone nanoparticles containing magnetite for magnetic drug carrier. *International Journal of Pharmaceutics*, vol. 324, no. 2, p. 185-190. [\[CrossRef\]](#)
- ZHAO, H.; GAGNON, J. and HAFELI, U.O. (2007). Process and formulation variables in the preparation of injectable and biodegradable magnetic microspheres. *Biomagnetic Research and Technology*, vol. 5, no. 1, p. 2. [\[CrossRef\]](#)

How to reference this article:

VILOS, C.; GUTIÉRREZ, M.; ESCOBAR, R.A.; MORALES, F.; DENARDIN, J.C.; VELÁSQUEZ, L. and ALTBIR, D. (2013). Superparamagnetic Poly(3-hydroxybutyrate-co-3-hydroxyvalerate) (PHBV) nanoparticles for biomedical applications. *Electronic Journal of Biotechnology*, vol. 16, no. 5. <http://dx.doi.org/10.2225/vol16-issue5-fulltext-8>